PCCP

Why does 2-(2-aminoethylamino)ethanol have superior CO2 separation performance to monoethanolamine?: A computational study

Journal:	*Physical Chemistry Chemical Physics*
Manuscript ID	CP-COM-03-2022-001136.R1
Article Type:	Communication
Date Submitted by the Author:	11-May-2022
Complete List of Authors:	Aso, Daiki; Kyushu University, Department of Molecular and Material Sciences, Interdisciplinary Graduate School of Engineering Sciences Orimoto, Yuuichi; Kyushu University, Department of Advanced Materials Science and Engineering, Faculty of Engineering Sciences Higashino, Makoto; Oita College, Department of Civil and Environmental Engineering, National Institute of Technology Taniguchi, Ikuo; Kyushu University, International Institute for Carbon-Neutral Research Aoki, Yuriko; Kyushu University, Faculty of Engineering Sciences, Department of Material Sciences

COMMUNICATION

Why does 2-(2-aminoethylamino)ethanol have superior CO_2 separation performance to monoethanolamine?: A computational study

Received 00th January 20xx,
Accepted 00th January 20xx

DOI: 10.1039/x0xx00000x

Daiki Aso,[a] Yuuichi Orimoto,[b] Makoto Higashino,[c] Ikuo Taniguchi [d] and Yuriko Aoki *[b]

Our computational reaction analysis shows that 2-(2-aminoethylamino)ethanol (AEEA) has superior performance to monoethanolamine for CO_2 separation, in terms of its ability to sorb CO_2 by the primary amine and desorb CO_2 by the secondary amine in AEEA.

Introduction

Recently, the global average temperature has been increasing, which has contributed to major problems such as rising sea and river levels,[1,2] abnormal weather conditions,[3,4] and adverse effects on ecosystems.[5] This increase in temperature is known to be caused by an increase in the concentration of carbon dioxide (CO_2) in the atmosphere.[6] However, many countries around the world depend heavily on coal-fired power plants that produce a large amount of CO_2; about 40 percent of the world's electricity is generated by coal combustion.[7,8] Because there are no alternatives that can be quickly, cheaply, and broadly deployed, society will likely remain dependent for some time on coal despite its substantial CO_2 emissions. Therefore, it is important to capture and store the exhausted CO_2 efficiently to prevent further contributions to global warming. Here, CO_2 separation from the exhaust gas (H_2/CO_2) of coal-based plants refers to the sorption and desorption of CO_2 using amine-containing solvents or membranes (see Fig. 1(a)).[8] Exhaust gases may contain not only H_2/CO_2 but also N_2 and other gases, but we focus on only H_2/CO_2 in this study. At the microscale, CO_2 sorption and desorption to amine corresponds to CO_2 interaction with and dissociation from amine, respectively. Fig. 1(a) shows a schematic image in which an amine-containing membrane allows CO_2 exhaust gas to pass through but blocks H_2. Monoethanolamine (MEA, $H_2N(CH_2)_2OH$) has been widely studied by experiments and theories as a model compound for CO_2 separation and capture.[9-11] More recently, 2-(2-aminoethylamino)ethanol (AEEA, $H_2N(CH_2)_2NH(CH_2)_2OH$) and diethylenetriamine (DETA, $H_2N(CH_2)_2NH(CH_2)_2NH_2$) have attracted attention for its superior CO_2 separation and capture performance compared to monoamines such as MEA.[12-15] In this study, we focused on AEEA for which a large amount of experimental data was reported.[12-14] AEEA is a diamine with a primary and a secondary amine group and a hydroxyl (-OH) group, as shown in Fig. 1(b). For simplicity, the primary and secondary amines of AEEA are referred to as $AEEA_p$ and $AEEA_s$, respectively. Our previous study showed that the structure of AEEA in its twisted form is more stable than that in its all-trans form.[16] Therefore, the twisted AEEA structure is assumed to be the reactant that interacts with CO_2 in this study.

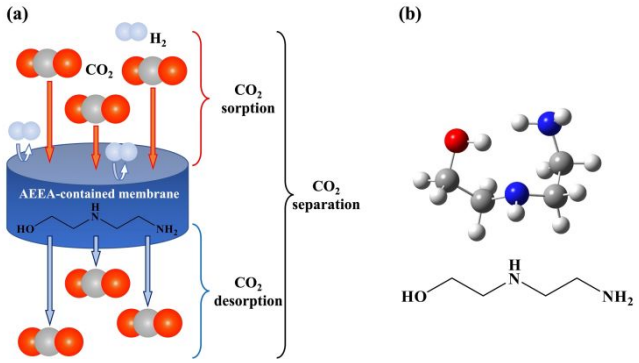

Fig. 1(a) Schematic image of CO_2 separation process by an AEEA-containing membrane. (b) Structure of twisted-form AEEA. Red, blue, gray, and white colors represent oxygen (O), nitrogen (N), carbon (C), and hydrogen (H) atoms, respectively.

[a] Department of Molecular and Material Sciences, Interdisciplinary Graduate School of Engineering Sciences, Kyushu University, 6-1 Kasuga-Park, Fukuoka 816-8580, Japan. E-mail: daiki.aso.736@s.kyushu-u.ac.jp
[b] Department of Advanced Materials Science and Engineering, Faculty of Engineering Sciences, Kyushu University, 6-1 Kasuga-Park, Fukuoka 816-8580, Japan. E-mail: orimoto.yuuichi.888@m.kyushu-u.ac.jp, aoki.yuriko.397@m.kyushu-u.ac.jp
[c] Department of Civil and Environmental Engineering, National Institute of Technology, Oita College, 1666 Maki, Oita 870-0152, Japan. E-mail: higasino@oita-ct.ac.jp
[d] International Institute for Carbon-Neutral Energy Research (WPI-I²CNER), Kyushu University, 744 Motooka, Nishi-ku, Fukuoka 819-0395, Japan. E-mail: ikuot@i2cner.kyushu-u.ac.jp

In our previous study,[16] we theoretically investigated CO_2 sorption reaction by the primary amine in AEEA according to experimental reports mentioning that the primary amine in AEEA reacts with CO_2 faster than the secondary one.[12,14] In Ref.16, we found that water (H_2O) molecules play an important role in promoting the reaction by causing ring-like protons transfer and creating H_3O^+ structure at the transition state. As a next step of our study, the present study compares the reaction mechanisms of CO_2 with the primary and secondary amines in AEEA and MEA using density functional theory (DFT) calculations to determine why AEEA exhibits superior CO_2 separation performance compared to MEA as found experimentally.[13,14] Historically, studies[16-18] have widely examined the sorption reactions of the primary amine including our previous study[16] but have not studied desorption reactions for either AEEA or MEA. The present study focuses on sorption but, in order to consider the complete CO_2 separation process, also discusses desorption.

AEEA is known to participate in two-step CO_2 reactions to form carbamic acid at each primary and secondary amine site via the following equations:[19]

Primary amine:

$$\mathrm{AEEA} + \mathrm{CO_2} + \mathrm{H_2O} \rightleftarrows \mathrm{AEEACOO_p^-} + \mathrm{H_3O^+}, \quad (1)$$

$$\mathrm{AEEACOO_p^-} + \mathrm{H_3O^+} \rightleftarrows \mathrm{AEEACOO_pH} + \mathrm{H_2O}. \quad (2)$$

Secondary amine:

$$\mathrm{AEEA} + \mathrm{CO_2} + \mathrm{H_2O} \rightleftarrows \mathrm{AEEACOO_s^-} + \mathrm{H_3O^+}, \quad (3)$$

$$\mathrm{AEEACOO_s^-} + \mathrm{H_3O^+} \rightleftarrows \mathrm{AEEACOO_sH} + \mathrm{H_2O}. \quad (4)$$

The first step reactions (Eqs. (1) and (3)) are the formation of a carbamate anion, while the second step reactions (Eqs. (2) and (4)) correspond to carbamate protonation.

Computational details

Reaction analyses based on DFT calculations were performed to investigate the reaction between $AEEA_p$/$AEEA_s$ and CO_2. All calculations were carried out using the Gaussian 16 program,[20] and calculation results were visualized by Gaussview 6.0.[21] In this study, we used the M06-2X[22] functional and 6-31+G(d,p) basis set. This functional is known to be effective for molecules in which noncovalent interactions play an important role.[22] Pruned 99,590 integration grid was used for all the M06-2X calculations to keep the computational accuracy. Solvent effects from water (dielectric constant: 78.36) were described using the integral equation formalism polarizable continuum model (IEF-PCM).[23,24] Transition state (TS) structures were searched to determine reaction pathways. The structures of reactant (RC) and product complexes (PC) were obtained by intrinsic reaction coordinate (IRC)[25] calculations from the TS structures, followed by full geometrical optimizations. Thermochemical analyses were carried out based on vibration analysis, and the energy was corrected by the temperature (358.15 K) and pressure (2.4 MPa) regarding the experiments of Kai *et al.*[26] Relative energies to the RC (not separated reactants) were used to show the stability of each state in the reaction pathway to keep the consistency with our previous study.[16]

Table 1. Gibbs free energy (ΔG) and total energy (ΔE) of activation in reaction pathways of CO_2 interaction with primary, secondary amines in AEEA, and primary amine in MEA.

	Step	ΔG (kcal/mol)	ΔE (kcal/mol)
Primary amine (AEEA)	**First (RC→INT 1)**	3.14	2.36
	Second (INT 1→INT 2)	-0.31	0.59
	Third (INT 2→PC)	6.29	10.07
Secondary amine (AEEA)	**First (RC→INT)**	3.95	1.88
	Second (INT→PC)	13.60	15.77
Primary amine (MEA)	**First (RC→INT)**	4.30	1.81
	Second (INT→PC)	10.75	13.38

Results and discussions

Calculations investigated the CO_2 interaction with twisted AEEA (see Fig. 1(b)) as the first stage of CO_2 separation. Fig. 2 shows the pathway for CO_2 interaction with $AEEA_p$, corresponding to Eqs. (1) and (2), which was found to be a three-step reaction by these calculations. In the first reaction step (from the RC to intermediate (INT) 1), $AEEA_p$ is attacked by CO_2 to form $AEEA(NH_2)_pCOO$. The -OH group and secondary amine form hydrogen bonds with H_2O in the RC structure. It is assumed that the H_2O molecule is captured by the -OH group according to our previous study.[16] Furthermore, CO_2 forms a covalent C-N bond (1.59 Å in length) with the primary amine in the INT 1 structure (see Fig. S1(a)). In addition, the orbital hybridization around the carbon (C) atom of the CO_2 changes from *sp* (RC) to incomplete sp^2 (INT 1) (Fig. S1(b)). We can consider that the first RC→INT 1 step is the middle stage of Eq. (1); that is, $AEEA(NH_2)_pCOO$ is formed as an intermediate before the formation of carbamate anion by deprotonation. The Gibbs free energy of activation (ΔG) from RC to INT 1 was found to be 3.14 kcal/mol (see Table 1). In the second step (INT 1→INT 2), the hydrogen bond between $AEEA_s$ and H_2O is broken and H_2O moves away from $AEEA_s$. Intermolecular hydrogen bonds

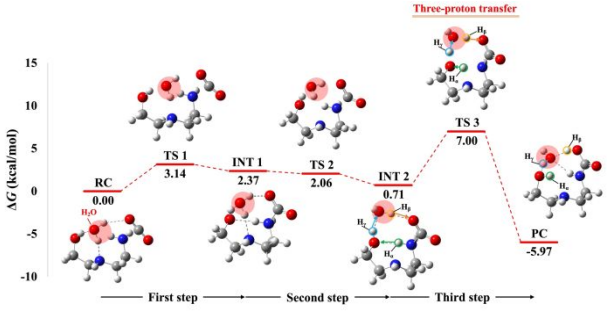

Fig. 2 Reaction pathway of the CO_2 interaction with $AEEA_p$ (Gibbs free energy, ΔG) at the M06-2X/6-31+G(d,p) level within the IEF-PCM. The green, yellow, and blue markers represent hydrogen atoms H_α, H_β, and H_γ, respectively.

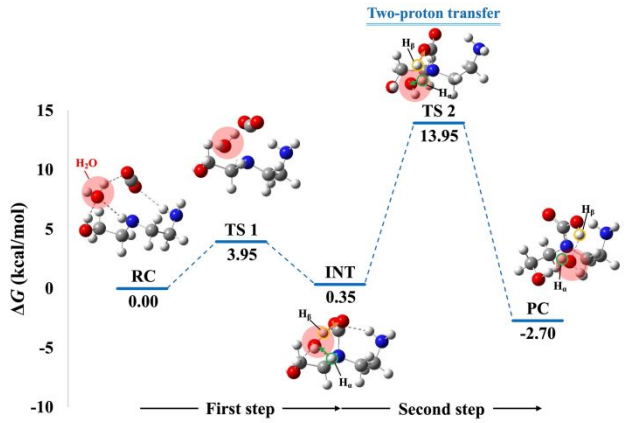

Fig. 3 Reaction pathway of the CO_2 interaction with the $AEEA_s$ (Gibbs free energy, ΔG) at the M06-2X/6-31+G(d,p) level within the IEF-PCM. See the caption of Fig. 2 regarding colored markers.

recombine in $AEEA(NH_2)_pCOO$ in this step, although it is not a carbamate anion. TS 2 is more stable than INT 1, and ΔG for this reaction step has a negative value of -0.31 kcal/mol (Table 1). However, Fig. S2 shows that this is an error due to temperature and pressure corrections. The total energy of activation (ΔE) without these corrections has a positive value of 0.59 kcal/mol (Table 1). The third step (INT 2→PC) includes three atomic movements: (i) the hydrogen (H) atom of the primary amine (H_α) in AEEA transfers to the -OH group; (ii) the H atom of the -OH group (H_γ) moves to H_2O; (iii) the H atom of H_2O (H_β) moves to CO_2. According to Ref. 16, the moving hydrogen atoms are protons, a fact confirmed by this study as well (see Table S1). The concerted movement of these three protons (H_α^+, H_β^+ and H_γ^+) around the $AEEA_p$ is referred to as "three-proton transfer" in this study. The movement of H_2O in the INT 1→INT 2 step is what is required to initiate the three-proton transfer. Here, movement (i) corresponds to deprotonation from $AEEA_p$. It can be seen in TS 3 that a hydronium ion (H_3O^+) is formed by H_2O and H_γ at INT 2. Based on previous work, it is known that activation energy decreases by forming H_3O^+ in the TS.[16] In the PC structure, the deprotonation from H_3O^+ causes the H_β movement to CO_2 (movement (iii)) to form carbamic acid, and the PC is much more stable than the RC, INT 1, and INT 2. This means that the deprotonation of $AEEA_p$ and the formation of carbamic acid through the three-proton transfer at the third step may contribute significantly to the stability of the PC structure. Moreover, orbital hybridization of the C atom of CO_2 changes from incomplete sp^2 in INT 2 to complete sp^2 in the PC (Fig. S1). Another H atom in $AEEA_p$ that is not transferred in TS 3 forms a hydrogen bond with H_2O. In the third step, the protonation of COO^- and the deprotonation of the $AEEA_p$ occur simultaneously. Thus, the last step corresponds to the reaction from the middle stage of Eq. (1) to (2). The activation energy of the third step is larger than that of the other steps, meaning that it is the rate-limiting process in the reaction.

Fig. 3 shows the reaction pathway of CO_2 interaction with $AEEA_s$. Based on these calculations, this is a two-step reaction. In the first step (RC→INT), $AEEA_s$ is attacked by CO_2 to form $AEEA(NH)_sCOO$. In the RC structure, H_2O is captured via hydrogen bonding by both the -OH group and $AEEA_s$. CO_2 forms a covalent bond with the $AEEA_s$ in the INT structure (C-N bond length = 1.60 Å) (Fig. S1(a)). In addition, the O-C-O angle changes from around 180° to 135° (Fig. S1(b)). Thus, during the RC→INT step, the orbital hybridization of the C atom of CO_2 changes from *sp* to incomplete sp^2, similar to the $AEEA_p$ case. The first step of the reaction can be considered as the middle stage in Eq. (3). As the result, $AEEA(NH)_sCOO$ is formed as an intermediate before the formation of the carbamate anion. ΔG for this reaction is 3.95 kcal/mol (see Table 1). The structure of the RC and INT have almost the same energy, and it is possible that the relatively high ΔG of TS 2 is due to the stability of INT. In the second step (INT→PC), the H atom of the secondary amine (H_α) is transferred to H_2O while the H atom of H_2O (H_β) is moved to CO_2 as shown in Fig. 3. In this study, the concerted movement of two protons (H_α^+ and H_β^+) around $AEEA_s$ is referred to as "two-proton transfer". H_3O^+ forms as part of TS 2, similar to the case of $AEEA_p$. Unlike the $AEEA_p$ case, H_3O^+ in TS 2 is formed only from H_2O and H_β in INT. It should be stressed that in TS 2, the -OH group is not directly involved in the proton transfer reaction, although it is indirectly related to the two-proton transfer because it plays a role in capturing H_2O in the RC. The bond between the C atom of CO_2 and the nitrogen (N) atom of the $AEEA_s$ is strengthened from INT, with a single bond of length 1.60 Å, to the PC with a 1.5-fold bond of length 1.36 Å (Fig. S1(a)). The orbital hybridization of the C atom in CO_2 was found to change from incomplete sp^2 in INT to complete sp^2 in the PC (see Fig. S1). The second step corresponds to reacting from the middle stage of Eq. (3) to Eq. (4) and to the third step of the $AEEA_p$ reaction. Carbamic acid forms in the PC, and its energy is more stable than the RC and INT. The ΔG of the second step is 9.65 kcal/mol higher than that of the first step (Table 1), indicating that the second step is rate-limiting, similar to the third step of $AEEA_p$ case.

The changes in Gibbs free energy during the two reaction pathways were compared (see Fig. S3); results suggest that $AEEA_p$ is about 7 kcal/mol more likely to react with CO_2 than $AEEA_s$ in their rate-limiting steps (Table 1). Thus, $AEEA_p$ has a higher CO_2 sorption performance than $AEEA_s$. According to the literature investigating the hydration reaction of CO_2, the charge of the oxygen atoms in CO_2 and H_2O grows more negative as the number of transferred protons increases, which is expected to stabilize the TS structure and decrease the activation energy of the hydration reaction.[27,28] Fig. S4 shows that the charges of the oxygen atoms in CO_2 and the -OH group in the $AEEA_p$ reaction TS structure are more negative than those in the $AEEA_s$ TS. As a result, the structure of the TS in the $AEEA_p$ reaction is stabilized, lowering the activation energy.

It should be noted again that CO_2 separation by amine-containing membranes consists of both sorption and desorption processes. In order to separate CO_2, it is necessary to both sorb and then desorb CO_2. From the calculation results of CO_2 interaction with AEEA, it is determined that $AEEA_p$ has a higher CO_2 sorption performance than $AEEA_s$. However, the PC structure from the $AEEA_p$ reaction is 5.56 kcal/mol more stable

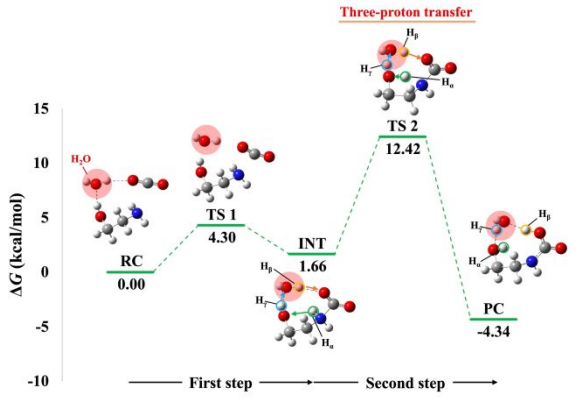

Fig. 4 Reaction pathway of the CO_2 interaction with the primary amine in MEA (Gibbs free energy, ΔG) at the M06-2X/6-31+G(d,p) level within the IEF-PCM. See the caption of Fig. 2 regarding colored markers.

than that of the $AEEA_s$ reaction (see Fig. S3). This difference can be explained by the mismatch in the H_2O chain and the strength of the hydrogen bonds (see Fig. S5). As a result, CO_2 dissociation from $AEEA_p$ is less likely to proceed compared to $AEEA_s$ because of the $AEEA_p$ reaction's stabilized PC structure. Thus, $AEEA_s$ shows superior CO_2 desorption performance to $AEEA_p$.

Reactions of CO_2 interaction with MEA by two-proton transfer have been well studied[11,17], but interaction with MEA by three-proton transfer has not been investigated. Fig. 4 shows CO_2 interaction with the primary amine of MEA. It can be seen that CO_2 forms a covalent bond with the primary amine of MEA in the first RC→INT step, and the three-proton transfer occurs in the second INT→PC step, similar to $AEEA_p$. The ΔG for this reaction is 10.75 kcal/mol, which is 4.46 kcal/mol greater than that for $AEEA_p$ but 2.85 kcal/mol less than that for $AEEA_s$ (see Table 1). That is, the order of CO_2 sorption ability can be considered as $AEEA_p$ > MEA > $AEEA_s$. Comparison of TS structures for CO_2 interaction with the $AEEA_p$ and MEA (Fig. S6) shows that H_α in $AEEA_p$ forms hydrogen bonds to two N atoms. On the other hand, H_α in MEA forms a hydrogen bond to a single N atom. In addition, hydrogen bonds (OH---H_2O, H_2O---COOH) of $AEEA_p$ are stronger than those of MEA (Fig. S6). These results suggest that the $AEEA_p$ reaction TS may be more stable than the MEA reaction TS due to strong hydrogen bonding. Thus, $AEEA_p$ is superior to MEA in CO_2 sorption performance. On the other hand, $AEEA_s$ is inferior to the primary amine of MEA in CO_2 sorption performance by the same reason as the difference between $AEEA_p$ and $AEEA_s$. Experiments reported CO_2 sorption ability with $AEEA_p$ > $AEEA_s$ at high CO_2 loading condition,[12,14] and faster CO_2 sorption of AEEA than MEA at the same condition.[13,14] Our results on CO_2 sorption performance agree in qualitative trend with the experiments by considering that the main contributor in AEEA to the CO_2 sorption is its primary amine.

Here, it is important to consider the energy change in RC formation stage from separated reactants (reactants→RC). As expected, in all the reaction paths enthalpy stabilizes RC by hydrogen bonds etc., while entropy destabilizes RC due to the reduction of randomness (see Table S2). By cancelling the opposite effects, the RC formation was found to be energetic destabilization process with approximately 6-9 kcal/mol.

The PC in the MEA reaction is 4.34 kcal/mol more stable than its RC (see Fig. 4). Meanwhile, the two PC structures in the $AEEA_p$ and $AEEA_s$ reactions are 5.97 and 2.70 kcal/mol more stable than their corresponding RC structures, respectively (see Figs. 2 and 3). Because the order of energy difference between the RC and PC (= RC − PC) is $AEEA_p$ > MEA > $AEEA_s$, the order of CO_2 desorption ability can be stated as $AEEA_s$ > MEA > $AEEA_p$. On the other hand, the PC is unstable than separated reactants before forming RC for all the reaction paths (see Table S3). However, the order of desorption ability predicted by the PC stability relative to reactants is consistent with the conclusion here based on the energy difference between the RC and PC. Because the rate-limiting step in the entire CO_2 separation reaction (sorption or desorption) can be affected by experimental conditions, two possible reaction conditions were considered (see Fig. S7). If the sorption process is rate-limiting, the order of CO_2 separation performance follows the sorption ability as $AEEA_p$ > MEA > $AEEA_s$. When the desorption is rate-limiting, CO_2 separation performance follows the desorption ability order as $AEEA_s$ > MEA > $AEEA_p$. Therefore, regardless of whether sorption or desorption acts as the rate-limiting factor, AEEA is superior to MEA in CO_2 separation performance by virtue of either the high sorption ability of $AEEA_p$ or the high desorption ability of $AEEA_s$.

Conclusions

In conclusion, we investigated the mechanism of CO_2 separation by $AEEA_p$, $AEEA_s$ and MEA using DFT. In the CO_2 interaction process, the reactions to generate carbamic acid were found to be rate-limiting for both primary and secondary amines. The results showed that the sorption performance is in the order of $AEEA_p$ > MEA > $AEEA_s$; for CO_2 desorption, the performance order is $AEEA_s$ > MEA > $AEEA_p$. Therefore, AEEA presents better CO_2 separation performance than MEA regardless of whether sorption or desorption is rate-limiting. We believe that this study elucidates the reaction mechanism of primary/secondary amines of AEEA and CO_2. This in turn can lead to the design of new CO_2 separation materials with higher efficiency than MEA, AEEA, and other currently used materials.

Acknowledgements

The authors sincerely thank Hisashi Yamauchi, Academic Research and Industrial Collaboration Management Office of Kyushu University for helpful discussions. This work was supported by the JSPS/MEXT (KAKENHI, Grant Nos. JP23245005, JP25810103, JP15KT0146, JP16K08321, JP16KT0059, JP20H00588, and JP21K12014), JST-CREST, and JST-SBIR. All calculations were performed on Linux PC systems in our laboratory and high-performance computing

systems at the Research Institute for Information Technology at Kyushu University.

Conflicts of interest

There are no conflicts to declare.

References

1 G. A. Meehl, W. M. Washington, W. D. Collins, J. M. Arblaster, A. Hu, L. E. Buja, W. G. Strand, H. Teng, Science, 2005, 307, 1769-1772.
2 M. Higashino, D. Aso, H. G. Stefan, Sci. Total Environ, 2021, 794, 148553.
3 A. R. Stine, P. Huybers and I. Y. Fung, Nature, 2009, 457, 435-440.
4 G. P. Yumul Jr., C. B. Dimalanta, N. T. Servando and N. A. Cruz, Clim. Change, 2013, 118, 715-727.
5 T. L. Root, J. T. Price, K. R. Hall, S. H. Schneider, C. Rosenzweigk and J. A. Pounds, Nature, 2003, 421, 57-60.
6 S. Manabe and R. T. Wetherald, J Atmos Sci, 1975, 32, 3-15.
7 J. Gibbins and Hannah Chalmers, Energy Policy, 2008, 36, 4317-4322.
8 M. E. Boot-Handford, et al., Energy Environ. Sci., 2014, 7, 130-189.
9 S. Kim, H. Shi, J. Y. Lee, Int. J. Greenh. Gas Control, 2016, 45, 181-188.
10 H. Yamada, J. Phys. Chem. B, 2016, 120, 10563-10568.
11 X. Yang, R. J. Rees, W. Conway, G. Puxty, Q. Yang and D. A. Winkler, Chem. Rev., 2017, 117, 9524-9593.
12 S. Ma'mun, J. P. Jakobsen and H. F. Svendsen, Ind. Eng. Chem. Res., 2006, 45, 2505-2512.
13 S. Ma'mun, V. Y. Dindore and H. F. Svendsen, Ind. Eng. Chem. Res., 2007, 46, 385-394.
14 I. Kim and H. F. Svendsen, Ind. Eng. Chem. Res., 2007, 46, 17, 5803-5809.
15 H.-T. Oh, J.-C. Lee and C.-H. Lee, Fuel, 2022, 314, 15, 122768.
16 D. Aso, Y. Orimoto, M. Higashino, I. Taniguchi and Y. Aoki, Chem. Phys. Lett., 2021, 783, 139070.
17 G. S. Hwang, H. M. Stowe, E. Paeka and D. Manogaranc, Phys. Chem. Chem. Phys., 2015, 17, 831-839.
18 C. Parks, E. Alborzi, M. Akram and M. Pourkashanian, Ind. Eng. Chem. Res., 2020, 59, 15214-15225.
19 C. Guo, S. Chen and Y. Zhang, Int. J. Greenh. Gas Control, 2014, 28, 88-95.
20 M. J. Frisch, et al., Gaussian 16, Revision C.01; Gaussian, Inc., Wallingford CT (2016).
21 R. D. Dennington II, T. A. Keith and J. M. Millam, GaussView, version 6.0.16, Semichem, Inc., Shawnee Mission KS (2016).
22 Y. Zhao and D. G. Truhlar, Theor. Chem. Account., 2008, 120, 215-241.
23 J. Tomasi, B. Mennucci and R. Cammi, Chem. Rev., 2005, 105, 8, 2999-3094.
24 A. V. Marenich, C. J. Cramer and D. G. Truhlar, J. Phys. Chem. B, 2009, 113, 18, 6378-6396.
25 K. Fukui, Acc. Chem. Res., 1981, 14, 12, 363-368.
26 T. Kai, S. Duan and F. Ito, Energy Procedia, 2017, 114, 613-620.
27 M. T. Nguyen, G. Raspoet, L. G. Vanquickenborne and P. T. Van Duijnen, J. Phys. Chem. A, 1997, 101, 40, 7379-7388.
28 M.-P. Gaigeot, A. Cimas, M. Seydou, J.-Y. Kim, S. Lee and J.-P. Schermann, J. Am. Chem. Soc., 2010, 132, 51, 18067-18077.